

Bentonite nanoclay-based drug-delivery systems for treating melanoma

FAEZEH HOSSEINI¹, FARZANEH HOSSEINI¹, SEYYED MEHDI JAFARI² AND AZADE TAHERI^{1,*}

¹ Novel Drug Delivery Systems Research Center, Department of Pharmaceutics, Faculty of Pharmacy, Isfahan University of Medical Sciences, Isfahan, Iran

² Department of Clinical Biochemistry, School of Pharmacy and Pharmaceutical Sciences, Isfahan University of Medical Sciences; Bioinformatics Research Center, Isfahan University of Medical Sciences, Isfahan, Iran

(Received 18 July 2017; revised 10 February 2018; Editor: George Christidis)

ABSTRACT: Local chemotherapy with biocompatible drug-delivery systems prolongs survival in patients. Due to the biocompatibility and high loading capacity, bentonite nanoclay is a good candidate for the fabrication of drug-delivery vehicles. In this study, doxorubicin-bentonite nanoclay complex (DOX-Bent complex) was prepared for the first time as a sustained-release drug-delivery system for intratumoural chemotherapy of melanoma. An efficient loading of DOX on 1 mg of bentonite nanoclay as high as $994.45 \pm 4.9 \mu\text{g}$ was obtained at a 30:1 DOX:bentonite nanoclay mass ratio. The DOX-Bent complex showed a low initial burst release of DOX in the first 24 h of release, followed by a sustained-release pattern for 21 days. The cumulative *in vitro* release of DOX from the DOX-Bent complex at pHs 6.5 and 7.4 revealed that the DOX-Bent complex can distinguish between tumour and normal tissues and express specific drug release at the tumour site. The results of cytotoxicity experiments indicated that the release pattern of DOX can supply sufficient DOX to inhibit growth of the melanoma cancer cell with an IC₅₀ of $0.29 \pm 0.07 \mu\text{g/mL}$. It is thus suggested that the DOX-Bent complex be introduced as a drug-delivery system for effective local cancer therapy.

KEYWORDS: bentonite nanoclay, biocompatible drug delivery, doxorubicin, melanoma, local chemotherapy, cytotoxicity.

Melanoma is one of the most aggressive skin cancers, responsible for almost 60% of lethal skin tumours (Bandarchi *et al.*, 2010). Among anti-cancer drugs, doxorubicin (DOX) is one of the more effective drugs against melanoma. However, doxorubicin resistance is a significant problem in the fight against melanoma and the adverse side effects of DOX on normal tissues, such as cardiotoxicity, myelosuppression, hair loss and nausea and vomiting limit its clinical use (Elliott & Al-Hajj, 2009). Local delivery of anti-cancer drugs to tumours can increase the availability of drug for

tumour uptake and simultaneously minimize drug resistance and systemic side effects (de Souza *et al.*, 2010). Recently, localized chemotherapy has attracted more attention than systemic chemotherapy for the treatment of most malignant solid tumours such as melanoma (Hanes *et al.*, 2001; Ta *et al.*, 2009; Krajišnik *et al.*, 2015; Hanif *et al.*, 2016; Pasbakhsh *et al.*, 2016; Liu *et al.*, 2016b). Experimental evidence has provided an important rationale for the development of a local drug-delivery system for DOX for the localized chemotherapy of melanoma. Nanoparticulate systems are attractive drug-delivery vehicles for localized and controlled delivery of chemotherapeutic agents to tumour sites (Wolinsky *et al.*, 2012). Nanoclays have drawn much attention as drug carriers

*E-mail: az.taheri@pharm.mui.ac.ir
<https://doi.org/10.1180/clm.2018.4>

due to their biocompatibility, safety, large specific surface area and large adsorption capacity of drugs (Patel *et al.*, 2006; Jafarbeglou *et al.*, 2016). For example, halloysite nanotubes are aluminosilicate nanoclay minerals which have been used as effective carriers for delivery of anti-cancer drugs to tumour sites. Halloysite nanotubes with modified surfaces with hydrophilic polymers showed promising potential for controlled delivery of anti-cancer drugs such as DOX and curcumin to the tumours (Liu *et al.*, 2016a; Yang *et al.*, 2016). Nanoclays are nanoparticles of layered silicate minerals ~ 1 nm thick and up to hundreds of nm wide and long (Patel *et al.*, 2006). Bentonite nanoclay is considered to be a very useful material for controlled drug delivery and surgical implants (Wei *et al.*, 2004; Zia *et al.*, 2011). Bentonite, which is composed predominantly of the smectite-group clay minerals, mainly montmorillonite, has a long history of use as an excipient (suspending agent, viscosifier, binder and emulsion stabilizer) in pharmaceutical formulations (Murray, 2007; Modabberi *et al.*, 2015). In addition to smectite, bentonite may contain other clay minerals such as kaolinite and some non-clay minerals such as quartz, feldspar, calcite, *etc.*, as impurities (Wright, 1968; Grim & Güven, 1978). As mentioned above, the main component of bentonite is smectite, which is responsible for the physical and chemical properties of bentonite. The smectite clay with a theoretical formula of $\text{Si}_8(\text{Al,Mg})_4\text{O}_{20}(\text{OH})_4 \cdot n\text{H}_2\text{O}$ has 2:1 layer structure with tetrahedral sheets bonded to octahedrally coordinated aluminium or magnesium atoms (Grim & Güven, 1978; Boyd, 1995). Smectite carries negative charge due to the substitution of Mg^{2+} for Al^{3+} ions in the octahedral sheets and the substitution of Al^{3+} for Si^{4+} in the tetrahedral sheet. The weak bonding between the 2:1 layers permits water and exchangeable cations to enter in the interlayer space leading to swelling of smectite. These cations and water molecules are attracted by the negative charge of smectite in the interlayer (Boyd, 1995).

Thus, water-soluble basic drugs may form complexes in their cationic form with smectite clay *via* electrostatic interactions (Takahashi & Yamaguchi, 1991a, 1991b). The electrostatic interactions between smectite-based nanoclay and drugs can be used to control the release of drugs from nanoclay by exchanging them with other ions present in the biological environment (Jafarbeglou *et al.*, 2016). Smectite may adsorb an amount of water up to ten times its weight, which separates the smectite layers effectively and disperses nanoclay in water and

biologic liquids homogeneously, facilitating their injection. In addition, nanoclays may restrict the invasion and migration of the cancer cells and thereby overcome cancer metastasis (Sposito *et al.*, 1999). These properties suggest that bentonite nanoclays have significant potential as drug-delivery systems for highly water-soluble basic drugs such as doxorubicin (DOX; molecular weight: 444.4). The excellent loading capacity and controlled-release properties of bentonite nanoclays may be exploited successfully for DOX delivery. The objective in the present study was to develop a bentonite nanoclay-based drug-delivery system for local delivery of DOX and to investigate its anti-cancer efficacy on melanoma tumour cells. To the best of the authors' knowledge, this is the first report on the development of a DOX-bentonite nanoclay complex which may be injected easily in and around the melanoma tumour site using routine syringes and needles to inhibit the melanoma cancer-cell proliferation. This drug-delivery system may be introduced as an effective means of local delivery of DOX to the melanoma tumour and may diminish the systemic side effects of the drug.

MATERIALS AND METHODS

Materials

A bentonite from the Mehredjan mine, Isfahan province, Iran, was used as the main raw material to produce the bentonite nanoclay. Doxorubicin hydrochloride was obtained from EBWE Pharm Ges.b.H. Nfg.KG A-4866 unterach, Austria. Thiazolyl blue tetrazolium bromide (MTT) was obtained from Merck Chemical Company (Germany). B16F10 melanoma cell line was purchased from the Pasteur Institute (Iran). Tripsin/EDTA, DMEM (Dulbecco's Modified Eagle Medium), RPMI (Roswell Park Memorial Institute medium), streptomycin/penicillin and FBS (foetal bovine serum) were purchased from Biosera Europe, ZI du Bousquet, France. Tween 80 was obtained from Merck-Schuchardt, Germany. Deionized water was used throughout the experiment. All other chemicals used were of analytical grade.

Preparation of bentonite nanoclay

The purification of the bentonite sample was performed using a hydrocyclone. The purified bentonite was ground with a high-speed vibration wet mill (HSVM, MM 200, Retsch Co. Ltd.) at 20 Hz at ambient temperature for 10 min. Milling was

performed using a vertical-type ball mill with a 1.5 L zirconia chamber, constant ball to powder weight ratio (40:1), 10 mm diameter zirconia balls, and a fixed rotational velocity of 200 rpm.

Preparation of DOX-Bent complexes

To prepare DOX-Bent complexes, 100 μL of bentonite nanoclay aqueous suspension (4 mg/mL) was added to 0.2, 0.4, 0.6, 0.8, 1, 2, 4 or 6 mL of DOX solution (2 mg/mL). The mass ratios of DOX per gram of bentonite nanoclay in the prepared mixtures were 1, 2, 3, 4, 5, 10, 20 and 30, respectively. The complexes obtained are denoted: DB-1:1, DB-1:2, DB-1:3, DB-1:4, DB-1:5, DB-1:10, DB-1:20 and DB-1:30. The samples were stirred with a magnetic stirrer at 600 rpm for 24 h at room temperature to form DOX-Bent complexes. After 24 h, the DOX-Bent complexes prepared were separated from unbound DOX molecules by centrifugation at 12,000 rpm for 10 min and the supernatants were collected. For complete separation of unbound DOX molecules from DOX-Bent complexes, 4 mL of deionized water was added to sediment and mixed thoroughly. Then, the prepared mixture was centrifuged to sediment the rinsed DOX-Bent complexes. The resulting supernatants passed through a 0.22 μm filter and the concentration of unbound fraction of the DOX was determined spectrophotometrically at 253 nm. All experiments were replicated at least three times. The amount of DOX physically bound to the 0.4 mg of bentonite nanoclay at different DOX:bentonite nanoclay mass

ratios was then calculated after three repetitions by the difference between the amount of DOX added to the bentonite nanoclay and the amount of unbound DOX, and presented as the average value of three repetitions (Table 1). Then, the DOX-Bent complexes were collected after centrifugation and their weight was measured precisely.

Determination of size and zeta potential of DOX-Bent complexes

The particle size and zeta potential of DOX-Bent complexes were measured using a Zetasizer 3600 instrument (Malvern Instrument Ltd, Worcestershire, UK) at 25°C, by dispersing 0.1 mg of the bentonite nanoclay or DOX-Bent complexes in 1 mL of deionized water.

Scanning Electron Microscopy (SEM)

The morphology of the bentonite nanoclay and DOX-Bent complex (DB-30:1) was studied using SEM (HITACHI S-4160 Tokyo, Japan) at an acceleration voltage of 20 kV. The bentonite nanoclay and DOX-Bent complex (DB-30:1) were dried at room temperature and coated with gold to prevent charging.

Fourier Transform Infrared Spectroscopy

The DOX, bentonite nanoclay and DOX-Bent complex (DB-30:1) were diluted with KBr and pressed into pellets. The FTIR spectra of samples

TABLE 1. Amounts of adsorbed DOX (μg) on the surface of 1 mg bentonite nanoclay and the size and zeta potential of prepared doxorubicin-bentonite nanoclay complexes (DOX-Bent) at different DOX: bentonite nanoclay mass ratios ($n = 3 \pm \text{SD}$).

Sample name	DOX/bentonite nanoclay mass ratio (wt:wt)	Particle size (nm)	Zeta potential (mV)	Amount of DOX attached (μg) on the surface of 1 mg of bentonite nanoclay
DB-1:1	1:1	154 \pm 3	-23.5	910.05 \pm 4.75
DB-2:1	2:1	231 \pm 3	-22.8	922.25 \pm 5.5
DB-3:1	3:1	294 \pm 5	-22.3	938.4 \pm 6.15
DB-4:1	4:1	321 \pm 2	-21.9	650.1 \pm 4.3
DB-5:1	5:1	355 \pm 7	-21.4	956.6 \pm 5.25
DB-6:1	6:1	413 \pm 3	-21.1	971.35 \pm 3.8
DB-10:1	10:1	427 \pm 6	-20.2	977.0 \pm 2.1
DB-20:1	20:1	467 \pm 3	-19.3	985.5 \pm 1.15
DB-30:1	30:1	481 \pm 2	-18.4	994.45 \pm 4.9

were recorded using an FTIR spectrometer (JASCO, FT/IR-6300, Japan) in the range 400–4000 cm^{-1} .

X-ray diffraction (XRD) analysis

The mineralogical composition of the original bentonite, the bentonite nanoclay and the DOX-Bent complex (DB-30:1) were studied by XRD using a Philips X'PERT X-ray diffractometer (Germany), with Cu anode, at 40 kV and 30 mA. The XRD data were collected at room temperature in the 2θ range 5–80°.

Determination of the release of DOX from DOX-Bent complexes in 0.2 M phosphate buffer at pH 7.4 and 6.5

The extracellular pH of tumour tissues has been shown to be more acidic (pH 6.5–7.0) than healthy tissues (pH 7.4) (Estrella et al., 2013). Thus, the release of DOX from DOX-Bent complexes was measured in 0.2 M phosphate buffer at pH levels of 7.4 (*i.e.* similar to the physiological pH value) and 6.5 (*i.e.* similar to the extracellular pH of solid tumours). To do this, 5 mg samples of DOX-Bent complexes were placed in a dialysis tube (cellulose membrane, cutoff 12,000 Da, Merck, Germany), and the dialysis tube was placed into a wide-mouth jar containing 45 mL of phosphate buffer containing 2% Tween 80 at the two pH levels (7.4 and 6.5) as the release medium. The temperature and stirring rate of the system were maintained at 37°C and 100 rpm, respectively. At predetermined time intervals, an aliquot of the release medium was withdrawn and the same volume of fresh medium was added back to the release medium. The concentration of DOX was quantified spectrophotometrically at 498 nm (UV mini/420 Shimadzu, Japan).

Injectability test of suspensions of DOX-Bent complexes

The injectability of the aqueous suspensions of DOX-Bent complexes (4 mg/mL) was determined using a compression mode of a texture analyzer (SANTAM®, Tehran, Iran). The injection forces from at least three measurements were obtained from STM Report Software. A 1 mL syringe was filled with DOX-Bent complexes suspension and a 26-gauge needle was attached to the syringe. The syringe plunger end was placed in contact with a load cell (500 N). Fresh chicken meat was used to simulate injection into subcutaneous tissue and muscle. The needle was

inserted to a depth of 2.5 cm under the chicken skin. The injection speed was set at 60 mm/min. The force applied to push the syringe plunger during the injection in the fresh chicken meat was reported as the injection force (Rungsevijitprapa & Bodmeier, 2009).

Cell culture

The highly metastatic mouse melanoma cell line, B16F10 cells, was purchased from the Pasteur Institute of Iran, Tehran. The cells were maintained in a humidified incubator with 5% CO_2 at 37°C. They were fed with Dulbecco's Modified Eagle Medium (DMEM) supplemented with 10% (v/v) Fetal Bovine Serum (FBS) and penicillin-streptomycin (100 IU/mL and 100 $\mu\text{g}/\text{mL}$, respectively).

Cell viability assay of B16F10 cells

The effect of DOX, bentonite nanoclay and DOX-Bent complexes on the viability of melanoma cancer cells was evaluated by MTT assay. B16F10 cells were seeded (1×10^4 cells/well) in a 96-well microplate and incubated overnight to allow cell attachment. Then, 20 μL of various concentrations (0.375, 0.75, 1.5, 3 and 6 $\mu\text{g}/\text{mL}$) of DOX was added to wells containing 180 μL of medium and incubated for 48 h. To evaluate the cytotoxic effect of the bentonite nanoclay on B16F10 cells, 20 μL of bentonite nanoclay suspension (4 mg/mL) was placed in wells of a 96-well plate containing 180 μL of medium and incubated for 48 h. To evaluate the cytotoxic effect of DOX-Bent complexes on B16F10 cells, 1 mg of DOX-Bent complex (DB-30:1) was diluted with various amounts of bentonite nanoclay aqueous suspension (4 mg/mL) until the 20 μL samples of the diluted DOX-Bent complexes suspensions prepared contained 0.375, 0.75, 1.5, 3 and 6 μg of DOX. Subsequently, 20 μL each of the diluted DOX-Bent complexes suspensions prepared were placed in wells of a 96-well plate. Then, 180 μL of medium were added to each well and incubated for 48 h. After 48 h, 20 μL of MTT solution (0.5 mg/mL) was added to each well and incubated for 4 h. Then, 150 μL of DMSO was added to dissolve the formazan crystals formed in each well and the absorbance values of each well was determined using a microplate reader (Bio-Rad Laboratories, Hercules, CA, USA) at 570 nm. The percentage of cell survival was calculated as the absorbance value of wells for treated cell to the absorbance value of wells for untreated cells (negative control). The experiments were repeated three times.

Statistical analysis

All enumerative analysis was carried out using *Statistical Package for the Social Sciences* version 20 software (SPSS Inc, Chicago, IL, USA). The statistical significance of differences was achieved *via* one-way analysis of variance (ANOVA). All cases were two-sided, and *P*-values <0.05 were assessed to be statistically significant. The consequences are demonstrated as mean \pm standard deviation.

RESULTS AND DISCUSSION

Zeta potential of DOX-Bent complexes at various DOX:bentonite nanoclay mass ratios

The bentonite nanoclay was utilized for the first time as the carrier in the current study due to its good biocompatibility, safety and high drug-loading capacity. The smectite particles in the nanoclay had a mean \pm SD hydrodynamic diameter of 115 ± 4 nm as measured by zetasizer and were negatively charged (zeta potential -24.8 ± 0.2 mV). Positively charged DOX molecules may adsorb onto the negatively charged surface of the smectite particles by electrostatic attraction (Fig. 1).

The change in surface charges of bentonite nanoclay after DOX attachment supports electrostatic interactions between DOX and smectite surfaces. The zeta potential of the nanoclay particles increased after surface modification with DOX molecules due to the neutralization of the negative charge of their surface. The increase in the zeta potential of the particles indicates that

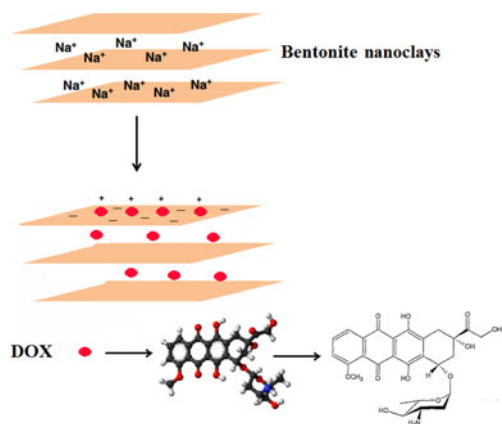


FIG. 1. Adsorption of the positively charged DOX molecules on the negatively charged surface of the smectite particles in the nanoclay by electrostatic attraction.

part of the negative charge of the nanoclay was neutralized by electrostatic interaction with positively charged groups of DOX molecules. With increasing amount of DOX added relative to a fixed amount of bentonite nanoclay, the amount of DOX attached on the nanoclay surface increased, thereby increasing the zeta potential of the nanoclay. The amounts of DOX molecules adsorbed on the surface of smectite nanoparticles at various DOX:bentonite nanoclay mass ratios are listed in Table 1.

The amount of DOX adsorbed on the surface of nanoclay particles increased with increasing amount of DOX in DOX-bentonite nanoclay complexes (Table 1). In addition, the particle size of the DOX-modified bentonite nanoclay increased with increasing amount of DOX-bentonite nanoclay complexes. Similar results were obtained in a previous study which showed an increase in the particle size of colloidal silica nanoparticles ($\sim 25\%$) after surface modification with 3-(trimethoxysilyl) propyl methacrylate (Yu *et al.*, 2003). The maximum amount of DOX adsorbed on the surface of nanoclay particles (994.45 ± 4.9 μg) was recorded after addition of 6 mg DOX to 1 mg of bentonite nanoclay (DB-30:1) (*cf.* Table 1), which is comparable to the amount of DOX adsorbed in DB-20:1 (DOX:bentonite nanoclay mass ratio = 20) (*p* value > 0.05). Thus, at the DOX:bentonite nanoclay mass ratio of 20, the surfaces of bentonite nanoclay became saturated with DOX and no additional DOX was adsorbed on the surfaces of smectite nanoparticles above the concentration of 150 mg/mL of DOX (Meira *et al.*, 2015). The large amount of DOX adsorbed on the surface of nanoclay due to the electrostatic interaction and hydrogen bonding between DOX and the nanoclay particles, means that the DOX molecules may be dispersed uniformly in the aqueous suspension of the bentonite nanoclay by simple stirring (Lee *et al.*, 2013). Because the largest amount of DOX molecules adsorbed on the surface of nanoclay particles was in DB-30:1, this formulation was selected as the optimum formulation for the remainder of this study.

XRD analysis

The XRD patterns of the original bentonite, the bentonite nanoclay and the DOX-Bent complex are given in Fig. 2. The original bentonite sample is composed mainly of smectite, with quartz, calcite, dolomite, albite, muscovite and clinoptilolite impurities (Fig. 2a). The presence of these impurities underlines the need for purification of the bentonite.

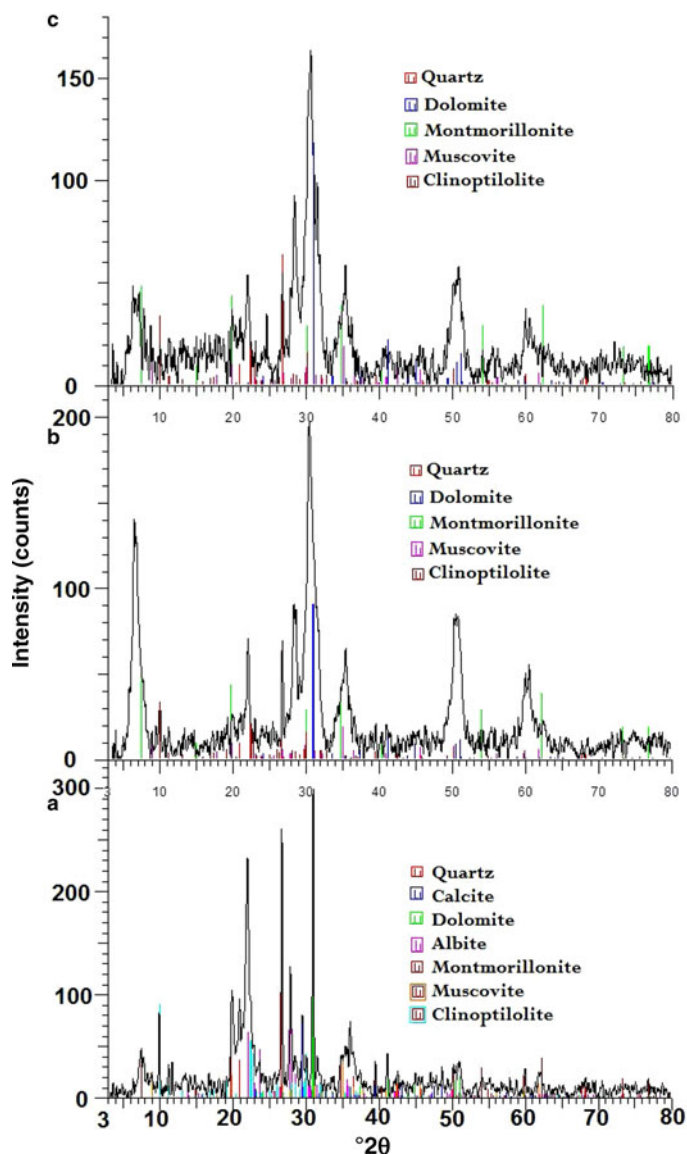


FIG. 2. XRD patterns of: (a) the original bentonites; (b) the bentonite nanoclay; and (c) the DOX-Bent complex.

The XRD pattern of purified bentonite (bentonite nanoclay) is free of calcite and albite (Fig. 2b). In addition, the intensity of the diffraction peaks of quartz, dolomite, muscovite and clinoptilolite impurities decreases, whereas that of smectite increases significantly compared with unpurified bentonite, suggesting that purification successfully decreased the abundance of impurities (Gong *et al.*, 2016). Also, in the XRD pattern of the DOX-Bent complex, the nature of smectite has not changed (Fig. 2c). Thus,

no chemical reaction occurred between the DOX and bentonite nanoclay (Li *et al.*, 2017).

Fourier Transform Infrared Spectroscopy

Fig. 3 presents the FTIR spectra of the DOX, bentonite nanoclay and the DOX-Bent complex (DB-30:1). In the FTIR spectrum of DOX (Fig. 3a), the principal absorption bands appeared at 1582.31 and 1618.95 cm^{-1} due to the N-H bending of primary

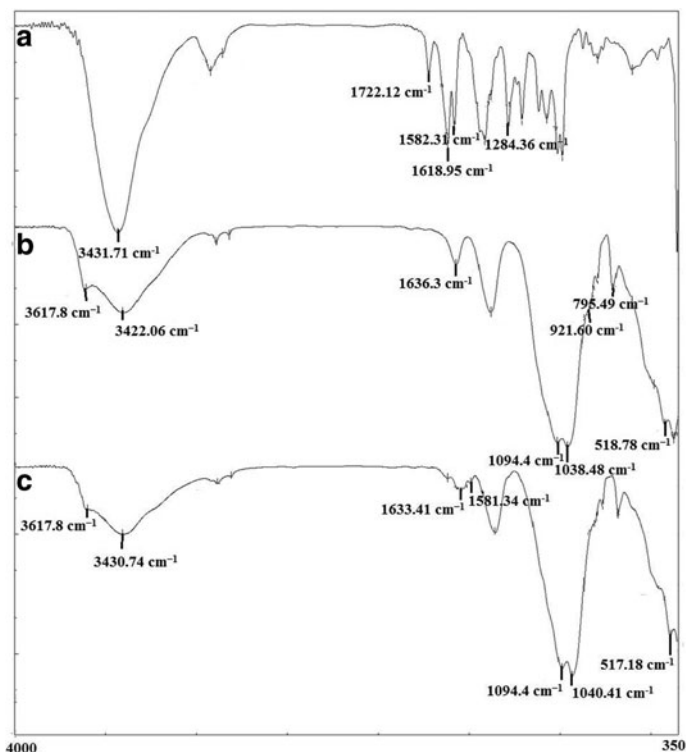


FIG. 3. FTIR spectra of: (a) the DOX; (b) the bentonite nanoclay; and (c) the DOX-Bent complex (DB-30:1).

amine group, at 1722.12 cm^{-1} due to C=O stretching vibration and at 1284.36 cm^{-1} due to C–O–C asymmetric stretching vibration. The broad band in the region $3100\text{--}3500\text{ cm}^{-1}$ indicates the N–H and O–H stretching vibrations (Kayal & Ramanujan, 2010; Chen *et al.*, 2015).

The FTIR spectra of the bentonite nanoclay (Fig. 3b) exhibited a broad band at 3422 cm^{-1} attributed to the OH-stretching mode of interlayer water. The characteristic bands at 1636 and 1094 cm^{-1} originate from the bending vibration of physically adsorbed water and a longitudinal Si–O stretching vibration, respectively. The bands at 3617 cm^{-1} (Al–OH and Mg–OH vibrations) and 922 cm^{-1} (Al–Al–OH bending vibration) are typical of dioctahedral smectites (Farmer, 1964). Other principal absorption bands appeared at 1038 and 795 cm^{-1} due to the Si–O bending and stretching of smectite and quartz, respectively. The band at 518 cm^{-1} is due to Al–O–Si bending vibrations (Farmer, 1964; Xu *et al.*, 2000).

The N–H stretching (3430 cm^{-1}) and N–H bending (1581 cm^{-1}) bands of DOX, the OH deformational

mode of water (1633 cm^{-1}) the longitudinal Si–O stretching vibration (1094 cm^{-1}), the Al–OH and Mg–OH vibrations (3617 cm^{-1}), the Si–O–Si bending vibration (1040 cm^{-1}) and the Al–O–Si bending vibration (517.18 cm^{-1}) present in the original bentonite nanoclay which also appeared in the spectra of the DOX-Bent complex (DB-30:1) (Fig. 3c) indicate the presence of DOX and bentonite nanoclay in the bentonite nanoclay complex (DB-30:1). The N–H stretching and N–H bending bands of DOX in the spectrum of the DOX-Bent complex (DB-30:1) shifted to lower wavenumbers and their intensity decreased compared with the DOX spectra (Fig. 3). Additionally, the bands of the OH deformational mode of water and the Si–O–Si stretching of DOX-Bent complex in DB-30:1 spectra became slightly broader and shifted to lower wavenumbers. These changes are attributed to the interactions between the functional groups of DOX (amine and hydroxyls) and the smectite particles (Ramanery *et al.*, 2013). Moreover, no new bands appeared in the spectrum of the DOX-Bent complex (DB-30:1).

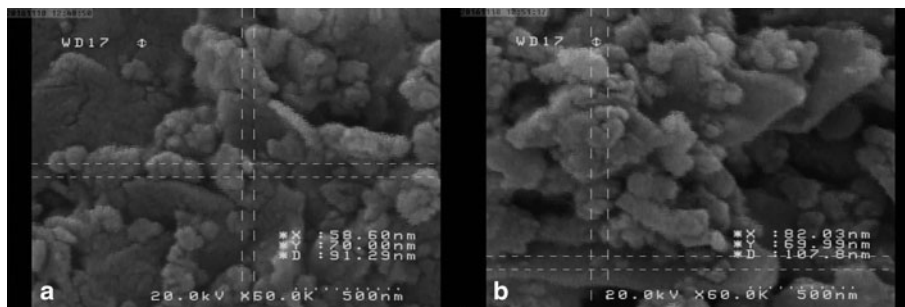


FIG. 4. SEM images of bentonite nanoclay (a) and a DOX-Bent complex (DB-30:1) (b).

Scanning Electron Microscopy

Scanning electron microscopy images of bentonite nanoclay and the DOX-Bent complex (DB-30:1) are shown in Fig. 4. The images show that the particles in the nanoclay and the DOX-Bent complex (DB-30:1) had irregular shapes. The nanoclay particles had diameters of 80–120 nm (mean diameter of 95 ± 10 nm). The average diameter of particles in the DOX-Bent complex (DB-30:1) increased slightly after surface modification with DOX (100–150 nm with mean diameter 130 ± 15 nm). These results suggest that the surface of nanoclay particles was modified successfully with DOX molecules. The increase in nanoparticle diameter after surface modification with various molecules has been reported in other studies (e.g. Mahdavi *et al.*, 2013).

The diameters of nanoclay particles and DOX-Bent complex particles determined by laser-light scattering were larger than those determined by SEM. It is suggested that laser-light scattering records the average hydrodynamic diameter of nanoparticles while SEM depicts the actual diameter of nanoparticles. Smaller sizes of nanoparticles determined by SEM compared with laser-light scattering have been reported in previous studies (Das *et al.*, 2005; Taheri *et al.*, 2011).

Release of DOX from the DOX-Bent complex at pH 7.4 and 6.5

To determine whether bentonite nanoclay may regulate the release of DOX, the release of DOX was investigated at pH values of 6.5 and 7.4 obtained for tumours and adjacent normal tissue in humans (Estrella *et al.*, 2013). The controlled-release patterns of DOX from the DOX-Bent suspension (DB-30:1) in phosphate buffer solutions with pH 7.4 and 6.5 are presented in Fig. 5. Under simulated normal

physiological conditions (pH 7.4), DB-30:1 showed a low DOX release rate, with a cumulative release of 13.25% over 4 days, which might be related to the strong electrostatic interactions between the positively charged DOX molecules and the negatively charged smectite surfaces at pH 7.4. Under acidic tumour pH (pH 6.5), DOX-Bent complex (DB-30:1) showed a faster DOX release rate, with a cumulative release of 20.66% over 4 days. At pH 6.5, partial protonation of AlOH groups of smectite particles may generate positive charges and reduce the surface charge of smectite and therefore the electrostatic interaction between the DOX molecules and bentonite nanoclay (Barany *et al.*, 2015). Thus, this reduced electrostatic interaction might increase the DOX release rate from DOX-Bent complex in cancerous tissues (pH 6.5), promote targeted delivery of DOX to cancerous tissues and diminish the side effects of DOX (Kim *et al.*, 2013). In the release profiles, significant initial burst release of DOX from DOX-bentonite nanoclay complex was not found; such behaviour may decrease

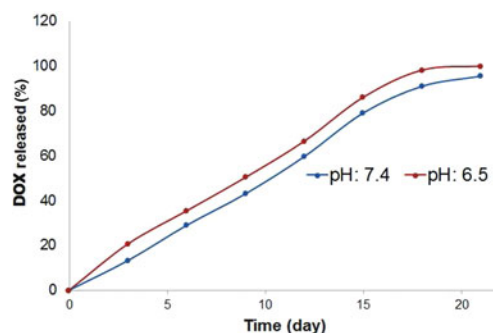


FIG. 5. Release patterns of DOX from DOX-Bent suspension (DB-30:1) in phosphate buffer solutions with pH 7.4 and 6.5.

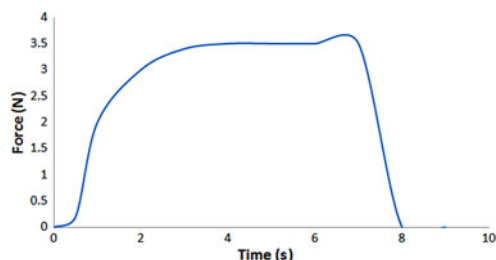


FIG. 6. Force required to expel the DOX-Bent complex aqueous suspension (4 mg/mL) through a 26-gauge needle from a 1 mL syringe.

the probability of harming normal cells. Moreover, the sustained release of DOX may increase the continued destruction of malignant melanoma cells in tumour tissue and improve the anti-tumour efficacy without additional toxic side effects (Mahdavi *et al.*, 2013).

Injectability of complex aqueous suspension of DOX-Bent

Because the DOX-Bent complex aqueous suspension (4 mg/mL) must be injected in and around the melanoma tumour site, the injectability characteristic of this suspension should be evaluated. The ease of injectability decreases the injection pain for patients and the injection fatigue for clinicians. The ease of injection may be shown by the required force needed to expel materials to the injection site. The force required to expel DOX-Bent complex aqueous suspension (4 mg/mL) through a 26-gauge needle from a 1 mL syringe is shown in Fig. 6. The maximum injection

force required was $\sim 3.5 \pm 0.22$ N. Formulations with the injection forces in the range of 0–10 N *in vitro* may be injected easily in tissues (Rungseevijitprapa & Bodmeier, 2009). Thus, no difficulty is expected in the injection of DOX-Bent complex aqueous suspension (4 mg/mL) in and around the melanoma tumour site.

Cell viability assay

An MTT cell viability assay was performed to determine the anti-cancer activity of DOX-Bent complexes. Bentonite nanoclay without DOX loading did not display any apparent cytotoxicity. After 48 h of incubation with 20 μ L of bentonite nanoclay suspension (4 mg/mL), $>99.15 \pm 1.01\%$ of B16F10 cells survived. The low cytotoxic effect of bentonite nanoclay on the B16F10 melanoma cancer cells could be explained by their hydrophilic surface and biocompatibility (Patel *et al.*, 2006; Jafarbeglou *et al.*, 2016). The cell-growth inhibition after 48 h of incubation for the free DOX and DOX-Bent complex (DB-30:1) is shown in Fig. 7. The modification of the surface of bentonite nanoclay with DOX significantly enhanced the cytotoxicity of bentonite nanoclay on the B16F10 cells (Fig. 7). The ANOVA test revealed that, at the same treatment dose, the DOX-Bent complex (DB-30:1) exhibited more anti-tumour activity on melanoma cancer cells than did the free DOX (P value <0.05). Free DOX and the DOX-Bent complex (DB-30:1) induced destruction of B16F10 melanoma cancer cells with IC_{50} (concentration that inhibits 50% of cell proliferation) values of 0.45 ± 0.12 and 0.22 ± 0.07 μ g/mL, respectively. Therefore the DOX-Bent

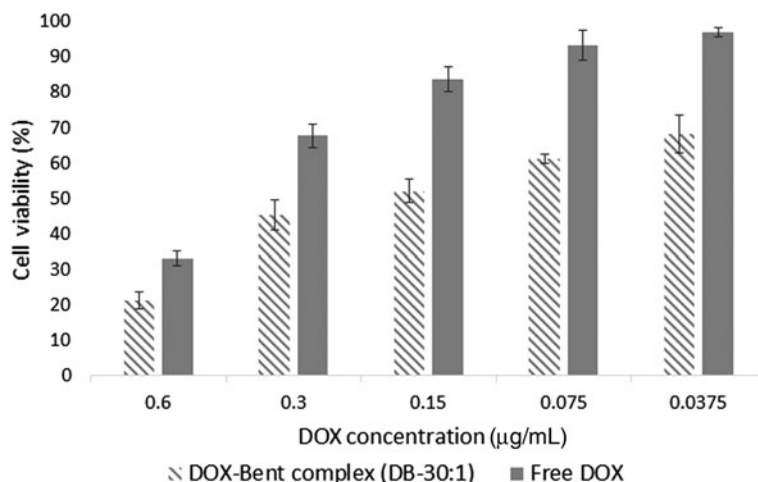


FIG. 7. Cell-growth inhibition after 48 h of incubation for the free DOX and DOX-Bent complex (DB-30:1).

complex (DB-30:1) was more cytotoxic to B16F10 cells than free DOX due to its capacity for the controlled release of DOX which may increase the continued destruction of malignant melanoma cells. Moreover, the anti-tumour efficacy of DOX did not decrease after adsorption on the surface of bentonite nanoclay. These findings suggest the feasibility of the local use of the DOX-Bent complex (DB-30:1) as an alternative source of free DOX due to its capacity for continuous release of DOX without losing its anti-cancer capability and with fewer systemic side effects (Salehi *et al.*, 2013).

CONCLUSION

In this study, a high loading and controlled release of DOX on bentonite nanoclay was investigated. With increasing loading of DOX on smectite particles, nanoclay complexes containing up to 1000 µg of DOX/mg of bentonite nanoclay were prepared. The DOX-Bent complex (DB-30:1) may be an effective compound for the localized chemotherapy of melanoma cancer. The DOX-Bent complex (DB-30:1) might be sterilized easily by autoclave and injected around and into tumours. The DOX-Bent complex (DB-30:1) may provide an appreciable cytotoxic effect against melanoma cancer cells and therefore may be introduced as a significant advance in localized chemotherapy.

ACKNOWLEDGMENTS

This project was supported by the Novel Drug Delivery Systems Research Center, Faculty of Pharmacy, Isfahan University of Medical Sciences, Isfahan, Iran (Research Grant No: 295202).

REFERENCES

- Bandarchi B., Ma L., Navab R., Seth A. & Rasty G. (2010) From melanocyte to metastatic malignant melanoma. *Dermatology Research and Practice*.
- Barany S., Meszaros R., Taubaeva R. & Musabekov K. (2015) Electro-surface properties of kaolin and bentonite particles in solutions of electrolytes and surfactants. *Colloid Journal*, **77**, 692–697.
- Boyd C.E. (1995) *Bottom Soils, Sediment, and Pond Aquaculture*. Springer Science & Business Media.
- Chen L., Xue Y., Xia X., Song M., Huang J. *et al.* (2015) A redox stimuli-responsive superparamagnetic nanogel with chemically anchored DOX for enhanced anticancer efficacy and low systemic adverse effects. *Journal of Materials Chemistry B*, **3**, 8949–8962.
- Das S., Banerjee R. & Bellare J. (2005) Aspirin loaded albumin nanoparticles by coacervation: implications in drug delivery. *Trends in Biomaterials and Artificial Organs*, **18**, 203–12.
- De Souza R., Zahedi P., Allen C.J. & Piquette-Miller M. (2010) Polymeric drug delivery systems for localized cancer chemotherapy. *Drug Delivery*, **17**, 365–375.
- Elliott A.M. & Al-Hajj M.A. (2009) ABCB8 mediates doxorubicin resistance in melanoma cells by protecting the mitochondrial genome. *Molecular Cancer Research*, **7**, 79–87.
- Estrella V., Chen T., Lloyd M., Wojtkowiak J., Cornell H. H. *et al.* (2013) Acidity generated by the tumor microenvironment drives local invasion. *Cancer Research*, **73**, 1524–1535.
- Farmer V. C. & Russell J. D. (1964) The infra-red spectra of layer silicates. *Spectrochimica Acta*, **20**, 1149–1173.
- Gong Z., Liao L., Lv G. & Wang X. (2016) A simple method for physical purification of bentonite. *Applied Clay Science*. **119**, 294–300.
- Grim R.E. & Güven N. (1978) *Bentonites: Geology, Mineralogy, Properties and Uses*, Elsevier, Amsterdam.
- Hanes J., Sills A., Zhao Z., Suh K.W., Tyler B., DiMeco F. *et al.* (2001) Controlled local delivery of interleukin-2 by biodegradable polymers protects animals from experimental brain tumors and liver tumors. *Pharmaceutical Research*, **18**, 899–906.
- Hanif M., Jabbar F., Sharif S., Abbas G., Farooq A. & Aziz M. (2016) Halloysite nanotubes as a new drug-delivery system: a review. *Clay Minerals*, **51**, 469–477.
- Jafarbeglou M., Abdouss M., Shoushtari A.M. & Jafarbeglou M. (2016) Clay nanocomposites as engineered drug delivery systems. *RSC Advances*, **6**, 50002–50016.
- Kayal S. & Ramanujan R.V. (2010) Doxorubicin loaded PVA coated iron oxide nanoparticles for targeted drug delivery. *Materials Science and Engineering: C*, **30**, 484–490.
- Kim I., Byeon H.J., Kim T.H., Lee E.S., Oh K.T., Shin B.S. *et al.* (2013) Doxorubicin-loaded porous PLGA microparticles with surface attached TRAIL for the inhalation treatment of metastatic lung cancer. *Biomaterials*, **34**, 6444–6453.
- Krajišnik D., Daković A., Malenović A., Kragović M. & Milić J. (2015) Ibuprofen sorption and release by modified natural zeolites as prospective drug carriers. *Clay Minerals*, **50**, 11–22.
- Lee Y., Jung G.E., Cho S.J., Geckeler K.E. & Fuchs H. (2013) Cellular interactions of doxorubicin-loaded DNA-modified halloysite nanotubes. *Nanoscale*, **5**, 8577–8585.
- Li X., Wu Z., He Y., Ye B.C. & Wang J. (2017) Preparation and characterization of monodisperse microcapsules with alginate and bentonite via external gelation

- technique encapsulating *Pseudomonas putida* Rs-198. *Journal of Biomaterials Science, Polymer Edition*, **28**, 1556–1571.
- Liu M., Chang Y., Yang J., You Y., He R., Chen T. & Zhou C. (2016a) Functionalized halloysite nanotube by chitosan grafting for drug delivery of curcumin to achieve enhanced anticancer efficacy. *Journal of Materials Chemistry B*, **4**, 2253–2263.
- Liu M., He R., Yang J., Long Z., Huang B., Liu Y. & Zhou C. (2016b) Polysaccharide-halloysite nanotube composites for biomedical applications: A review. *Clay Minerals*, **51**, 457–467.
- Mahdavi M., Ahmad M.B., Haron M.J., Namvar F., Nadi B., Rahman M.Z.A. & Amin J. (2013) Synthesis, surface modification and characterisation of biocompatible magnetic iron oxide nanoparticles for biomedical applications. *Molecules*, **18**, 7533–7548.
- Meira S.M.M., Jardim A.I. & Brandelli A. (2015) Adsorption of nisin and pediocin on nanoclays. *Food Chemistry*, **188**, 161–169.
- Modabberi S., Namayandeh A., López-Galindo A., Viseras C., Setti M. & Ranjbaran M. (2015) Characterization of Iranian bentonites to be used as pharmaceutical materials. *Applied Clay Science*, **116–117**, 193–201.
- Murray H.H. (2007) Bentonite applications. Pp. 85–110 in: *Applied Clay Mineralogy: Occurrences, Processing and Applications of Kaolins, Bentonites, Palygorskite-sepiolite, and Common Clays*. Developments in Clay Science, **2**. Elsevier, Amsterdam.
- Pasbakhsh P., De Silva R., Vahedi V. & Churchman J.G. (2016) Halloysite nanotubes: prospects and challenges of their use as additives and carriers – A focused review. *Clay Minerals*, **51**, 479–487.
- Patel H.A., Somani R.S., Bajaj H.C. & Jasra R.V. (2006) Nanoclays for polymer nanocomposites, paints, inks, greases and cosmetics formulations, drug delivery vehicle and waste water treatment. *Bulletin of Materials Science*, **29**, 133–145.
- Ramanery F.P., Mansur A.A. & Mansur H.S. (2013) One-step colloidal synthesis of biocompatible water-soluble ZnS quantum dot/chitosan nanoconjugates. *Nanoscale Research Letters*, **8**, 512.
- Rungsevijitprapa W. & Bodmeier R. (2009) Injectability of biodegradable in situ forming microparticle systems (ISM). *European Journal of Pharmaceutical Sciences*, **36**, 524–531.
- Salehi R., Irani M., Rashidi M.R., Aroujalian A., Raisi A., Eskandani M. *et al.* (2013) Stimuli-responsive nanofibers prepared from poly (N-isopropylacrylamide-acrylamide-vinylpyrrolidone) by electrospinning as an anticancer drug delivery. *Designed Monomers and Polymers*, **16**, 515–527.
- Spósito G., Skipper N.T., Sutton R., Park S.H., Soper A.K. & Greathouse J.A. (1999) Surface geochemistry of the clay minerals. *Proceedings of the National Academy of Sciences*, **96**, 3358–3364.
- Ta H.T., Dass C.R., Larson I., Choong P.F. & Dunstan D.E. (2009) A chitosan hydrogel delivery system for osteosarcoma gene therapy with pigment epithelium-derived factor combined with chemotherapy. *Biomaterials*, **30**, 4815–4823.
- Taheri A., Atyab F., Nouri F.S., Ahadi F., Derakhshan M. A., Amini M. *et al.* (2011) Nanoparticles of conjugated methotrexate-human serum albumin: preparation and cytotoxicity evaluations. *Journal of Nanomaterials*, **5**. doi: 10.1155/2011/768201.
- Takahashi T. & Yamaguchi M. (1991a) Host-guest interaction between swelling clay minerals and poorly water-soluble drugs. 1: Complex formation between a swelling clay mineral and griseofulvin. *Journal of Inclusion Phenomena and Macrocyclic Chemistry*, **10**, 283–297.
- Takahashi T. & Yamaguchi M. (1991b) Host-guest interactions between swelling clay minerals and poorly water-soluble drugs: II. Solubilization of griseofulvin by complex formation with a swelling clay mineral. *Journal of Colloid and Interface Science*, **146**, 556–564.
- Wei M., Shi S., Wang J., Li Y. & Duan X. (2004) Studies on the intercalation of naproxen into layered double hydroxide and its thermal decomposition by in situ FT-IR and in situ HT-XRD. *Journal of Solid State Chemistry*, **177**, 2534–2541.
- Wolinsky J.B., Colson Y.L. & Grinstaff M.W. (2012) Local drug delivery strategies for cancer treatment: gels, nanoparticles, polymeric films, rods, and wafers. *Journal of Controlled Release*, **159**, 14–26.
- Wright P.C. (1968) Meandu Creek bentonite – A reply. *Journal of the Geological Society*, **15**, 347–350.
- Xu W., Johnston C.T., Parker P. & Agnew S.F. (2000) Infrared study of water sorption on Na-, Li-, Ca-, and Mg-exchanged (SWy-1 and SAz-1) montmorillonite. *Clays and Clay Minerals*, **48**, 120–131.
- Yang J., Wu Y., Shen Y., Zhou C., Li Y.F., He R.R. & Liu M. (2016) Enhanced therapeutic efficacy of doxorubicin for breast cancer using chitosan oligosaccharide-modified halloysite nanotubes. *ACS Applied Materials & Interfaces*, **8**, 26578–26590.
- Yu Y. Y., Chen C. Y. & Chen W.C. (2003) Synthesis and characterization of organic-inorganic hybrid thin films from poly (acrylic) and monodispersed colloidal silica. *Polymer*, **44**, 593–601.
- Zhang M., Lu Y., Li X., Chen Q., Lu L., Xing M. *et al.* (2010) Studying the cytotoxicity and oxidative stress induced by two kinds of bentonite particles on human B lymphoblast cells in vitro. *Chemico-Biological Interactions*, **183**, 390–396.
- Zia K.M., Zuber M., Barikani M., Hussain R., Jamil T. & Anjum S. (2011) Cytotoxicity and mechanical behavior of chitin-bentonite clay based polyurethane bio-nanocomposites. *International Journal of Biological Macromolecules*, **49**, 1131–1136.